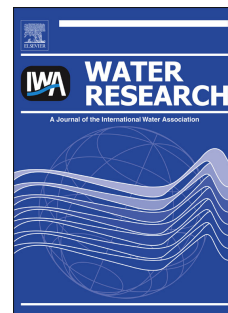


## Accepted Manuscript

Title: Model-based energy optimisation of a small-scale decentralised membrane bioreactor for urban reuse

Authors: Bart Verrecht, Thomas Maere, Lorenzo Benedetti, Ingmar Nopens, Simon Judd



PII: S0043-1354(10)00323-4

DOI: [10.1016/j.watres.2010.05.015](https://doi.org/10.1016/j.watres.2010.05.015)

Reference: WR 8010

To appear in: *Water Research*

Received Date: 11 November 2009

Revised Date: 7 May 2010

Accepted Date: 11 May 2010

Please cite this article as: Verrecht, B., Maere, T., Benedetti, L., Nopens, I., Judd, S. Model-based energy optimisation of a small-scale decentralised membrane bioreactor for urban reuse, *Water Research* (2010), doi: [10.1016/j.watres.2010.05.015](https://doi.org/10.1016/j.watres.2010.05.015)

This is a PDF file of an unedited manuscript that has been accepted for publication. As a service to our customers we are providing this early version of the manuscript. The manuscript will undergo copyediting, typesetting, and review of the resulting proof before it is published in its final form. Please note that during the production process errors may be discovered which could affect the content, and all legal disclaimers that apply to the journal pertain.

# 1 Model-based energy optimisation of a small-scale 2 decentralised membrane bioreactor for urban reuse

3 *Bart Verrecht\**, *Thomas Maere\*\**, *Lorenzo Benedetti\*\**, *Ingmar Nopens\*\** and *Simon Judd\*<sup>1</sup>*

4 \*Centre for Water Science, Cranfield University, Cranfield, Bedfordshire MK43 0AL, UK

5 \*\*BIOMATH, Department of Applied Mathematics, Biometrics and Process Control, Ghent  
6 University, Coupure Links 653, B-9000 Gent, BE

7 <sup>1</sup>Corresponding author: [s.j.judd@cranfield.ac.uk](mailto:s.j.judd@cranfield.ac.uk)

8

## 9 Abstract

10 The energy consumption of a small-scale membrane bioreactor, treating high strength  
11 domestic wastewater for community level wastewater recycling, has been optimised using a  
12 dynamic model of the plant. ASM2d was chosen as biological process model to account for  
13 the presence of phosphate accumulating organisms. A tracer test was carried out to  
14 determine the hydraulic behaviour of the plant. To realistically simulate the aeration demand,  
15 a dedicated aeration model was used incorporating the dependency of the oxygen transfer  
16 on the mixed liquor concentration and allowing differentiation between coarse and fine  
17 bubble aeration, both typically present in MBRs. A steady-state and dynamic calibration was  
18 performed, and the calibrated model was able to predict effluent nutrient concentrations and  
19 MLSS concentrations accurately. A scenario analysis (SCA) was carried out using the  
20 calibrated model to simulate the effect of varying SRT, recirculation ratio and DO set point on  
21 effluent quality, MLSS concentrations and aeration demand. Linking the model output with  
22 empirically derived correlations for energy consumption allowed an accurate prediction of the  
23 energy consumption. The SCA results showed that decreasing membrane aeration and SRT  
24 were most beneficial towards total energy consumption, while increasing the recirculation  
25 flow led to improved TN removal but at the same time also deterioration in TP removal. A  
26 validation of the model was performed by effectively applying better operational parameters  
27 to the plant. This resulted in a reduction in energy consumption by 23% without  
28 compromising effluent quality, as was accurately predicted by the model. This modelling  
29 approach thus allows the operating envelope to be reliably identified for meeting criteria  
30 based on energy demand and specific water quality determinants.

31

32 *Keywords:* Energy, Reuse, Model-based optimisation, Scenario analysis, MBR calibration

## 33 Symbols and abbreviations

34	<i>AOTR</i>	Actual oxygen transfer rate in $\text{gO}_2\cdot\text{d}^{-1}$
35	<i>ASM2d</i>	Activated sludge model no.2d
36	<i>BOD<sub>5</sub></i>	5 day biological oxygen demand in $\text{mg}\cdot\text{l}^{-1}$
37	<i>BOD<sub>f</sub></i>	5 day biological oxygen demand of a sample filtered through $0.45\ \mu\text{m}$ , in $\text{mg}\cdot\text{l}^{-1}$
38	<i>b<sub>PAO</sub></i>	Rate constant for lysis of <i>X<sub>PAO</sub></i> in $\text{d}^{-1}$
39	<i>CAS</i>	Conventional activated sludge
40	<i>COD</i>	Chemical oxygen demand in $\text{mg}\cdot\text{l}^{-1}$
41	<i>COD<sub>f</sub></i>	Chemical oxygen demand of a sample filtered through $0.45\ \mu\text{m}$ in $\text{mg}\cdot\text{l}^{-1}$
42	<i>C<sub>rsat_average</sub></i>	Average dissolved oxygen saturation concentration in $\text{gO}_2\cdot\text{m}^{-3}$ , for clean water 43 in an aeration tank for a given temperature <i>T</i>
44	<i>C<sub>ssat</sub></i>	Dissolved oxygen saturation concentration in $\text{gO}_2\cdot\text{m}^{-3}$ , in clean water at 20 °C 45 and 1 atm
46	<i>CSTR</i>	Continuously stirred tank reactor
47	<i>C<sub>tank</sub></i>	Actual oxygen concentration in the aeration tank in $\text{gO}_2\cdot\text{m}^{-3}$
48	<i>DO</i>	Dissolved oxygen in $\text{mgO}_2\cdot\text{l}^{-1}$
49	<i>F</i>	Correction factor for fouling of the air diffusers (1 for clean diffusers)

50	$F_{coarse}$	Correction factor for fouling of the coarse bubble air diffusers (1 for clean diffusers)
51		
52	$F_{fine}$	Correction factor for fouling of the fine bubble air diffusers (1 for clean diffusers)
53		
54	$HRT$	Hydraulic retention time in hours
55	$K_O$	Half saturation coefficient for oxygen, in $mgO_2 \cdot l^{-1}$
56	$MBR$	Membrane bioreactor
57	$MLSS$	Mixed liquor suspended solids in $mg \cdot l^{-1}$
58	$NH_4-N$	Ammonia-nitrogen in $mgN \cdot l^{-1}$
59	$NO_2-N$	Nitrite-nitrogen in $mgN \cdot l^{-1}$
60	$NO_3-N$	Nitrate-nitrogen in $mgN \cdot l^{-1}$
	$O_{air}$	Fraction of oxygen in the air in %
61	$ON$	Organic nitrogen in $mgN \cdot l^{-1}$
	$OTE$	Oxygen transfer efficiency in $m^{-1}$
62	$OTE_{coarse}$	Coarse bubble oxygen transfer efficiency in $m^{-1}$
63	$OTE_{fine}$	Fine bubble oxygen transfer efficiency in $m^{-1}$
64	$PO_4-P$	Ortho-phosphate in $mgP \cdot l^{-1}$
	$Q_{air}$	Airflow rate in $Nm^3 \cdot h^{-1}$
65	$Q_{air,coarse}$	Coarse bubble airflow rate in $Nm^3 \cdot h^{-1}$
66	$Q_{air,fine}$	Fine bubble airflow rate in $Nm^3 \cdot h^{-1}$
67	$S_A$	Fermentation products, considered to be acetate, in $mgCOD \cdot l^{-1}$
68	$SCA$	Scenario analysis
69	$S_F$	Fermentable, readily biodegradable organic substrates in $mgCOD \cdot l^{-1}$
70	$S_I$	Inert soluble organic material in $mgCOD \cdot l^{-1}$
71	$S_{NH4}$	Ammonium plus ammonia nitrogen in $mgN \cdot l^{-1}$
72	$SOTR$	Standard oxygen transfer rate in $gO_2 \cdot d^{-1}$
73	$S_{PO4}$	Inorganic soluble phosphorus, primarily ortho-phosphates in $mgP \cdot l^{-1}$
74	$SRT$	Solids retention time in days
75	$SS$	Suspended solids in $mg \cdot l^{-1}$
76	$T$	Temperature of the mixed liquor in $^{\circ}C$
77	$tCOD$	Total COD in $mg \cdot l^{-1}$
78	$TKN$	Total Kjeldahl nitrogen in $mgN \cdot l^{-1}$
79	$TN$	Total nitrogen in $mgN \cdot l^{-1}$
80	$TON$	Total oxidised nitrogen in $mgN \cdot l^{-1}$
81	$TP$	Total phosphorous in $mgP \cdot l^{-1}$
82	$X_H$	Heterotrophic organisms in $mgCOD \cdot l^{-1}$
83	$X_I$	Inert particulate organic material in $mgCOD \cdot l^{-1}$
84	$X_S$	Slowly biodegradable substrates in $mgCOD \cdot l^{-1}$
	$y$	Aerator depth in m
85	$Y_{PO}$	Polyphosphate (PP) requirement for storage of poly-hydroxy-alkanoates (PHA), in $gP \cdot (gCOD)^{-1}$
86		
87	$\alpha$	Clean-to-process water correction factor for oxygen transfer
88	$\beta$	Salinity surface tension correction factor, dimensionless
89	$\mu_{PAO}$	Maximum growth rate of $X_{PAO}$ in $d^{-1}$
	$\rho_{air}$	Density of air at standard conditions in $kg \cdot m^{-3}$
90	$\varphi$	Temperature correction factor for oxygen transfer
91	$\omega$	$\alpha$ -factor exponent coefficient, dimensionless

## 92 1 Introduction

93 Membrane bioreactors (MBR) offer a low-footprint option with high quality effluent for  
94 recycling municipal wastewater. For applications at small community level, small MBRs are  
95 required (Fletcher *et al.*, 2007; Gniirrs *et al.*, 2008, Abegglen *et al.*, 2008), which are then  
96 inherently less energetically efficient due to wide variations in flows and commensurately  
97 large peak loading factors demanding more conservative design. Given that the energy  
98 demand contributes significantly to the running costs, it is important to optimise process  
99 energy consumption to make the technology more competitive (Judd, 2006).

100  
101 Mathematical models are widely recognized as providing a useful tool for optimising  
102 biological treatment, and several semi-empirical models for the optimisation of MBRs are  
103 described in literature (Verrecht *et al.*, 2008; Wen *et al.*, 1999; Yoon *et al.*, 2004). These  
104 models, however, have limited predictive power regarding biological performance and total  
105 energy demand under dynamic conditions, or else focus mainly on sludge production. The  
106 activated sludge models (ASMs) by Henze *et al.* (2000), created with the purpose of  
107 describing the biological dynamics of conventional activated sludge (CAS) systems, have  
108 been successfully used in the past to optimise full scale CAS plants (Dochain and  
109 Vanrolleghem, 2001). However, literature on the application of the activated sludge models  
110 to full scale MBR is scarce or not readily accessible (Erftverband, 2001; Erftverband, 2004),  
111 and research focuses mainly on sludge production through application of ASM1 and ASM3 to  
112 lab and pilot scale MBR (Sperandio and Espinosa, 2008; Lubello *et al.*, 2009). The  
113 requirement for full scale validation of the ASM models for MBR applications has recently  
114 been identified as an urgent research need (Fenu *et al.*, 2010). Applying these ASM to MBRs  
115 demands that the differences between MBR and CAS systems be recognised, viz.: a)  
116 microbiological composition, leading to different stoichiometric and kinetic parameters (*inter*  
117 *alia* Wen *et al.*, 1999; Jiang *et al.*, 2005; Lobos *et al.*, 2005), b) biomass concentration,  
118 leading to changes in oxygen transfer and uptake (Krampe and Krauth, 2003; Germain *et al.*,  
119 2007), and c) requirement for additional aeration for membrane scouring (Judd, 2006).

120  
121 In this paper, the application of ASM2d to a small community-scale MBR for reuse has been  
122 appraised with the key objective of optimising energy demand without compromising nutrient  
123 removal. The study uses the BIOMATH calibration protocol (Vanrolleghem *et al.*, 2003),  
124 proceeding through a hydraulic characterisation of the system and employing both steady  
125 state and dynamic model calibration to predict water quality. The paper thus provides a case  
126 study of the calibration and application of ASM2d to a community-scale MBR. The MBR  
127 model incorporates an aeration model accounting for oxygen mass transfer at the operational  
128 biomass concentration and differentiates between coarse and fine bubble aeration. Energy  
129 consumption values for the different unit processes are derived empirically. A scenario  
130 analysis is conducted to link the predicted biological performance for different operational  
131 parameters with the empirically derived energy consumption values. The scenario analysis  
132 thus allows identification of better operational parameters, and the predicted energy saving  
133 and biological removal performance are verified on the full scale plant.

## 135 2 Materials and Methods

### 136 2.1 Plant description

137 The wastewater recycling plant produces an average reclaimed water flow of  $25 \text{ m}^3 \cdot \text{d}^{-1}$  for  
138 toilet flushing and irrigation (Figure 1). Domestic wastewater from the residences is collected  
139 via a pumping station and septic tanks, which provide buffering volume and primary settling.  
140 Influent from the septic tanks flows through 3 mm screens to the MBR, which contains both  
141 anoxic and aerobic zones for nitrification and denitrification respectively (Table 1). Although  
142 no anaerobic tank is provided, some of the influent phosphorous is biologically removed,  
143 suggesting that part of the anoxic tank may be (intermittently) anaerobic. The membrane

144 separation step is provided by 2 x 3 ZW500c (GE Zenon, Canada) membrane modules with  
145 a total membrane surface area of 139 m<sup>2</sup>, submerged in the aerobic zone.

## 146 147 2.2 Hydraulic profile

148 A tracer test was carried out using a 22.1 g spike of LiCl dosed into the anoxic zone, with  
149 samples taken from the anoxic to aerobic tank overflow weir, the effluent and the sludge  
150 recirculation loop every 20 to 30 minutes for the next 40 hours (corresponding to ~1.5 times  
151 the hydraulic residence time, HRT). Samples were analysed for Li by atomic emission  
152 spectroscopy at 670.784 nm (iCAP 6500 Dual View; Thermo Scientific). To validate the  
153 results and determine the number of tanks in series according to the tanks-in-series model  
154 (Levenspiel, 1998), the MBR was implemented (Figure 1) as an anoxic tank followed by an  
155 MBR unit (aerated tank with submerged membrane modules) in the modelling and simulation  
156 platform WEST<sup>®</sup> (MOSTforWATER N.V., Kortrijk, Belgium; Vanhooren *et al.*, 2003). Both  
157 tanks were assumed to be completely mixed. During the tracer test, the plant was run under  
158 normal flow conditions (Table 1).

## 159 160 2.3 Influent characterisation

161 The MBR was fed with domestic wastewater without rainwater dilution from dwellings with  
162 average water consumption of 80-100 l/capita<sup>-1</sup>.d<sup>-1</sup>. The wastewater strength was thus high  
163 (Table 2), and comparable to values reported for a single household MBR by Abegglen *et al.*  
164 (2008). The septic tanks were estimated to remove 20-30% of the COD, and 0-10% of the N  
165 and P (VSA, 2005), as well as buffering the variations in influent concentration to the benefit  
166 of biological performance (Gnirss *et al.*, 2008).

167  
168 Table 3 compares the community wastewater characterised according to the STOWA  
169 protocol (Roeleveld and van Loosdrecht, 2002) to data for a typical wastewater (Henze *et al.*,  
170 1999), and indicates this wastewater to be 48%, 324% and 81% higher in concentrations of  
171 total COD, TKN and TP respectively. The relative quantity of readily biodegradable  
172 substrates ( $S_F$  and  $S_A$ ) is also higher due to hydrolysis in the septic tanks (Zaveri and Flora,  
173 2002), which enhances bio-P removal for which the presence of fermentation products such  
174 as acetate ( $S_A$ ) is required (Henze *et al.*, 1999; Gernaey and Jørgensen, 2004). Flow variation  
175 was between 0 and 1.8 m<sup>3</sup>.hr<sup>-1</sup>, with substantially larger loads (up to 25%) over the weekend  
176 (Figure 2).

## 177 178 2.4 Steady state and dynamic plant modelling using ASM2d

179 For the steady state and dynamic simulations of the plant, ASM2d was chosen as the bio-  
180 chemical model since it includes enhanced biological P removal in addition to COD and N  
181 removal (Henze *et al.*, 1999). To obtain better representation of P removal, the ASM2d  
182 biomass decay rates modifications proposed by Gernaey and Jørgensen (2004) were  
183 adopted.

184  
185 For the model calibration, influent, mixed liquor and effluent data was taken collected from  
186 January till May 2009, totalling 93 days, which corresponds to approximately twice the SRT  
187 (47 days). A steady-state calibration of the full model was performed based on average data  
188 over this period (Table 2), and a DO set point of 2 mg.l<sup>-1</sup> was used, reflecting the average DO  
189 value in the aerobic zone. For the dynamic calibration, a high frequency measurement  
190 campaign was carried out, and an influent file was produced through analysis of SCADA  
191 data, containing a data recorded every 15 minutes for 93 days for the following parameters:  
192 influent flow, influent COD, COD<sub>f</sub>, BOD<sub>5</sub>, TSS, NH<sub>4</sub>-N, TKN, PO<sub>4</sub>-P, TP, recirculation flow,  
193 DO value and wastage flow. During the sampling period, the temperature ranged from 15.8  
194 to 20.7 °C. A number of process upsets occurred over this period, such as a mixer failure,  
195 resulting in a necessary manual increase in the recirculation flow to keep the anoxic zone

196 mixed and a blower failure resulting in low DO levels for a number of days. These upsets  
197 were included in the model.

198  
199 Since the model predictions were used for energy consumption calculations, the use of an  
200 adequate aeration model was of utmost importance. Basic aeration models, such as the one  
201 used in Benchmark Simulation Model 1 (BSM1, Copp, 2002) and many ASM model  
202 applications do not account for the detrimental effect of elevated MLSS concentrations on  
203 oxygen transfer, and control the oxygen transfer rate by controlling the oxygen transfer  
204 coefficient  $k_L a$ :

$$205 \quad SOTR = k_L a \cdot (DO - DO_{sat}) \cdot V \quad (1)$$

To account for the effect of elevated MLSS concentrations on oxygen transfer and for other dependencies of oxygen transfer, e.g., the difference in oxygen transfer from coarse and fine bubble aeration, typical for MBR, a more extensive model as described in Maere *et al.* (2009) was used (Metcalf and Eddy, 2003; Henze *et al.*, 2008; Verrecht *et al.*, 2008, Krampe and Krauth, 2003; Germain *et al.*, 2007, Stenstrom and Rosso, 2008), viz:

$$206 \quad AOTR = SOTR \cdot \frac{(\beta \cdot C_{rsat\_average} - C_{tank})}{C_{ssat}} \cdot \phi^{(T-20)} \cdot \alpha \cdot F \quad (2)$$

$$SOTR = 24 \cdot Q_{air} \cdot \rho_{air} \cdot OTE \cdot y \cdot O_{air} / 10000 \quad (3)$$

$$207 \quad \alpha = e^{-\omega \cdot MLSS} \quad (4)$$

In this model the influence of MLSS concentration on the AOTR is accounted for through the  $\alpha$ -factor (Eq. 4), and the effect of using different types of diffusers for biological and membrane aeration can be incorporated by calculating the SOTR for each type of diffuser individually, with appropriate values of oxygen transfer efficiency ( $OTE$ ) and fouling factor  $F$ . More details about the aeration model can be found in Maere *et al.* (2009).

## 208 209 2.5 Scenario analysis

210 A scenario analysis (SCA) was carried out to determine the optimum operating conditions by  
211 varying the experimentally-adjustable degrees of freedom (DOF) that were regarded as  
212 having the greatest impact on effluent quality and energy consumption:

- 213 • SRT: 9 values for the wastage rate, equally spaced between 0.1 to 2.278  $m^3 \cdot d^{-1}$   
214 yielding SRT values ranging from 10 to 228.7 days
- 215 • Recirculation rate: 9 values, equally spaced between 28.8  $m^3 \cdot d^{-1}$  to 187.2  $m^3 \cdot d^{-1}$   
216 (upper range of recirculation pump) yielding recirculation ratios to the influent flow of  
217 1.13 to 7.78
- 218 • Dissolved oxygen set point: 5 values, equally spaced between 0.75 and 2  $mg \cdot l^{-1}$

219  
220 For inputting to the SCA, a data set containing 35 days of influent was taken from the plant  
221 when operating under normal influent conditions. The scenario analysis was duplicated using  
222 two different membrane aeration rate values (84 and 42  $Nm^3 \cdot h^{-1}$ ), corresponding to the  
223 maximum and minimum realistic values for coarse bubble air flow ( $Q_{air,coarse}$ ), since this  
224 parameter accounts for a large part of the total energy consumption.

225  
226 The SCA grid, using the values described above, resulted in 486 different scenarios. The  
227 impact on activated sludge aeration, nutrient removal and MLSS concentration was studied.  
228 To calculate the energy consumption for each degree of freedom, empirical correlations for  
229 energy consumption of the unit processes (membrane aeration, biology aeration,  
230 recirculation pumping, permeate pumping and mixing) were derived from measurements on  
231 the plant, at an MLSS of 8,000  $mg \cdot l^{-1}$ . Membrane aeration energy was 0.029 to 0.034  
232  $kWh \cdot Nm^{-3}$  for  $Q_{air,coarse}$  of 84 and 42  $Nm^3 \cdot h^{-1}$  respectively, indicating that the blower becomes

233 less efficient at lower air flow rates. Energy demand for the recirculation pump varied linearly  
 234 with the flow rate, up to a maximum of  $0.037 \text{ kWh}\cdot\text{m}^{-3}$  of sludge pumped. Since the activated  
 235 sludge blower for biology aeration is controlled by an on/off controller at around  $2 \text{ mgO}_2\cdot\text{l}^{-1}$  (or  
 236 around the different DO set points, as described above) and runs at fixed speed when in  
 237 operation, the energy consumption per  $\text{Nm}^3$  is constant at  $0.0289 \text{ kWh}\cdot(\text{Nm}^3)^{-1}$ . For the  
 238 scenario analysis, the mixing energy was considered constant at  $4.6 \text{ kWh}\cdot\text{d}^{-1}$ . Since mixing  
 239 accounts for less than 5% of the total energy demand, changes in mixing energy arising from  
 240 changes in viscosity at different MLSS concentrations were considered negligible. The  
 241 permeate pump was constantly running at  $1.8 \text{ m}^3\cdot\text{h}^{-1}$  when in operation, resulting in an  
 242 energy consumption of  $0.056 \text{ kWh}\cdot\text{m}^{-3}$  of permeate. Sludge handling costs were ignored  
 243 since these depend on site-specific sludge management strategies.  
 244

### 245 3 Results and discussion

#### 246 3.1 Hydraulic profile

247 Figure 3 displays measured versus predicted Li concentrations in the anoxic and aerobic  
 248 zone during the tracer test. The correlation between the measured and predicted data for  
 249 both the anoxic and aerobic zone corroborates the assumption of perfect mixing. The  
 250 recovery of Li, defined as the ratio of Li added to Li recovered in the effluent, determined  
 251 through integration of the effluent Li flux, was 87%, and would have been higher for an  
 252 extended campaign. The measured Li concentrations in the effluent were always about  $7.5 \pm$   
 253  $3.5\%$  lower than the Li concentrations measured in the recirculation sludge, suggesting some  
 254 Li adsorption onto the flocs arose but not to a significant extent. The tanks could thus each  
 255 be considered CSTRs for the remainder of the modelling exercise.  
 256

#### 257 3.2 Model calibration

##### 258 3.2.1 Steady state calibration

259 A steady state calibration was performed to achieve an accurate simulation of the MLSS  
 260 concentration, this being instrumental in correctly predicting the aeration energy demand due  
 261 to its effect on oxygen transfer (via the  $\alpha$ -factor). However, as shown in Table 4, using default  
 262 values as reported by Henze *et al.* (1999) for all stoichiometric and biokinetic parameters,  
 263 leads to an underestimation of sludge production (MLSS concentration) by about 15%, as the  
 264 growth of  $X_{PAO}$  (and consequently bio-P removal) could not be simulated correctly in steady  
 265 state. This can be attributed to the fact that anaerobic conditions, required for the growth of  
 266  $X_{PAO}$ , do not occur during steady state simulation, indicating the need for a dynamic  
 267 calibration taking into account the influent variations. In steady state, a correct representation  
 268 of MLSS concentrations could only be achieved by making substantial and unrealistic  
 269 changes to  $\mu_{PAO}$  ( $2 \text{ d}^{-1}$  vs. default value of  $1 \text{ d}^{-1}$ ),  $b_{PAO}$  ( $0.1 \text{ d}^{-1}$  vs. default value of  $0.2 \text{ d}^{-1}$ ) and  
 270  $Y_{PO}$  ( $0.2 \text{ gP}\cdot(\text{g COD})^{-1}$  vs. default value of  $0.4 \text{ gP}\cdot(\text{g COD})^{-1}$ ) (Table 4).  
 271

##### 272 3.2.2 Dynamic calibration

273 When the dynamic influent file was applied to the model, the concentration of  $X_{PAO}$  started to  
 274 increase without the adjustments to  $\mu_{PAO}$ ,  $b_{PAO}$  and  $Y_{PO}$  that were necessary in the steady  
 275 state calibration. Upon reaching dynamic equilibrium, MLSS concentrations were  
 276 represented accurately using the default parameter values as reported by Henze *et al.*  
 277 (1999), thereby eliminating the need to adjust  $\mu_{PAO}$ ,  $b_{PAO}$  and  $Y_{PO}$  as was necessary under  
 278 steady-state conditions.  
 279

280 To calibrate the aeration model, the measured  $Q_{air, fine}$  (averaged over a 15 minute period)  
 281 was used as the input for the aeration model, while  $Q_{air, coarse}$  was fixed at  $84 \text{ Nm}^3\cdot\text{h}^{-1}$ , to mimic  
 282 the prevailing operational conditions during the calibration period. The values for  $OTE_{fine}$   
 283 ( $0.045 \text{ m}^{-1}$ ),  $OTE_{coarse}$  ( $0.015 \text{ m}^{-1}$ ) were taken from Metcalf and Eddy (2003), the value for  $\omega$   
 284 ( $0.084$ ) was the mean value derived from the data of Germain *et al.* (2007), Krampe and

285 Krauth (2003), and Metcalf and Eddy (2003).  $F_{coarse}$  (0.8) and  $F_{fine}$  (0.8) were calibrated to  
286 closely match the measured DO profile. Calibrating the fouling factors could be justified since  
287 an inspection of the diffusers had shown visible fouling. Moreover, more advanced  
288 techniques for measuring the  $\alpha$ -factor and  $OTE_{coarse}$  and  $OTE_{fine}$  were unavailable.  
289

290 Despite the plant upsets during the evaluated period, the used parameter set allowed for a  
291 satisfactory reproduction of the  $NH_4$ -N,  $NO_3$ -N and MLSS concentration trajectories; Figure 4  
292 compares the simulated nitrogen removal profiles ( $NH_4$ -N and  $NO_3$ -N) and MLSS  
293 concentrations with concentrations measured during an intensive sampling period on Days  
294 61-62 of the 93 day campaign. Predicted  $NH_4$ -N concentrations were consistently slightly  
295 higher than the measured values ( $\sim 0.25 \text{ mg}\cdot\text{l}^{-1}$  simulated vs  $\sim 0.04 \text{ mg}\cdot\text{l}^{-1}$  measured and  
296 confirmed by using two different analytical techniques). MBRs tend to achieve more stable  
297 and complete nitrification than CAS systems (Munz *et al.*, 2008), a fact that is apparently not  
298 well incorporated into the various CAS ASM models. Despite this shortcoming, when looking  
299 at the total nitrogen removal, the prediction is still very accurate (Figure 4). Predicted  $PO_4$ -P  
300 concentrations show acceptable values and dynamic behaviour (Figure 5) though  
301 consistently a few hours ahead of those measured. It is postulated that this is caused by the  
302 oversimplification of the actual hydraulics by the tanks-in-series concept, which may be  
303 unable to accurately predict the occurrence of localised anaerobic zones under certain  
304 conditions. However, a CFD model study and on-line data at different locations in the tank  
305 would be required to confirm this. In general it can be concluded that the calibrated model  
306 predicts nutrient and MLSS concentrations accurately using the default values for ASM2d  
307 (Henze *et al.*, 1999) and its modification (Gernaey and Jørgensen, 2004), and the model  
308 used along with the energy demand calculations in the subsequent scenario analysis.  
309

### 310 3.2.3 On/off controller for aeration model for predictive $Q_{air,fine}$ values in energy profiling

311 To lend predictive value to the model, the fine bubble aeration flow rate ( $Q_{air,fine}$ ) demanded  
312 an extra on/off controller, switching on aeration at  $DO < 1.5 \text{ mg}\cdot\text{l}^{-1}$  with  $Q_{air,fine}$  at  $90 \text{ Nm}^3\cdot\text{h}^{-1}$   
313 and switching off at  $DO > 2.5 \text{ mg}\cdot\text{l}^{-1}$ , simulating the actual blower operation at the plant. The  
314 integral of the predicted  $Q_{air,fine}$  value was within 3% difference from the actual measured  
315 value when using the parameters as calibrated in Section 3.2.2, indicating that aeration  
316 demand could be predicted accurately through this approach. Nutrient and MLSS  
317 concentrations were reproduced well, with predicted values generally well within 10% of the  
318 measured ones (Figure 4 and Figure 5). Any differences can be attributed to slight deviations  
319 from reality using the implemented on/off controller.  
320

### 321 3.3 Scenario analysis

322 The evolution of biological aeration demand and maximum effluent  $NH_4$ -N concentration as a  
323 function of the SRT (Figure 6) demonstrates that lowering the SRT by increasing the  
324 wastage rate has a beneficial effect on demand for  $Q_{air,fine}$ . However, Figure 6 also shows  
325 that this also leads to higher maximum effluent  $NH_4$ -N concentrations, indicating a trade-off  
326 between minimising the aeration demand (and thus energy consumption) and achievable  
327 effluent quality. Operation at SRTs below 23 days leads to a deterioration in nitrification,  
328 because of a decrease in MLSS and autotrophs concentration, and to an increase in F/M  
329 ratio, similar to observations by Cicek *et al.* (2001). Lowering the DO setpoint had a similar  
330 but less pronounced effect on nitrification.  
331

332 There is a similar phenomenon regarding phosphate and nitrate (Figure 7), in that an  
333 increase in the recirculation ratio leads to respectively lower and higher effluent  $NO_3$ -N and  
334  $PO_4$ -P concentrations. This arises because the denitrification and bio-P removal processes  
335 compete for the same carbon source (Metcalf and Eddy, 2003) and anaerobic conditions is  
336 less sustainable at higher recirculation ratios.  
337



338 Figure 8 shows that a change in the SRT (through variation in wastage rate), and thus MLSS  
 339 concentration, has a much larger impact on total aeration energy demand than changing the  
 340 recirculation ratio. At a DO setpoint of  $1.25 \text{ mg l}^{-1}$  and fixed recirculation ratio, the total fine  
 341 bubble aeration demand ( $Q_{air, fine}$ ) can change by up to 342% depending on the wastage rate,  
 342 while this change is limited to 44% when varying the recirculation ratio at fixed SRT and DO  
 343 set point. This confirms the importance of incorporating the MLSS dependency of the oxygen  
 344 transfer into the aeration model. The model thus allows the operating envelope to be  
 345 identified for meeting criteria based on energy demand and/or specific water quality  
 346 determinants.

347  
 348 It is acknowledged that over the range of operating conditions studied in the SCA, the  
 349 biological processes and kinetics may change. For instance, Sperandio and Espinosa (2008)  
 350 suggest that at elevated SRT some of the influent  $X_i$  should be considered as  $X_s$ , which has  
 351 implications on the overall sludge balance. Also, simultaneous nitrification and denitrification  
 352 may occur at low DO set points. The model accounts for this by using oxygen half-saturation  
 353 coefficients  $K_O$  for  $X_H$  and  $X_{PAO}$ . The effect of floc size on the value of  $K_O$  is still debated, the  
 354 small flocs of an MBR compared to those from CAS would be expected to yield lower values  
 355 for the halfsaturation constants (*inter alia* Manser *et al.*, 2005). However, no clear consensus  
 356 has been reached on the impact of specific operational conditions on kinetics. Hence, rather  
 357 than varying the biokinetic parameters in the model over the studied range of operational  
 358 parameters, all biokinetic parameters were assumed constant, and an *a posteriori* model  
 359 validation carried out by confronting the obtained model predictions of the scenario analysis  
 360 with experimental data independent of the calibration data set (Section 3.4).

361  
 362 The outcomes of the scenario analysis were linked with the empirical energy consumption  
 363 calculations, and ranked in terms of energy consumption while compliant with effluent quality  
 364 standards of  $<0.5 \text{ mg l}^{-1} \text{ NH}_4\text{-N}$ ,  $<20 \text{ mg l}^{-1} \text{ TN}$   $< 20 \text{ mg l}^{-1}$ , and  $5,000 \text{ mg l}^{-1}$  minimum MLSS.  
 365 Since reuse regulations - such as the US EPA guidelines for unrestricted urban reuse (EPA,  
 366 2004) - generally do not include stringent  $\text{NH}_4\text{-N}$  or TN guidelines, these parameters were  
 367 chosen to achieve consistent effluent quality under conservative operating conditions that  
 368 could be achieved in a real system.

369  
 370 When comparing the different parameter sets for the two studied air flow rates displayed, the  
 371 average energy consumption was  $13.1 \pm 4.7\%$  lower at a membrane coarse bubble aeration  
 372 of  $42 \text{ Nm}^3\text{h}^{-1}$  compared to  $84 \text{ Nm}^3\text{h}^{-1}$ . The maximum difference in energy consumption  
 373 between simulations for the different membrane airflow values was 28%, while the minimum  
 374 was 4.6%. When the membrane aeration airflow rate was set at  $42 \text{ Nm}^3\text{h}^{-1}$ , the minimum and  
 375 maximum predicted energy consumption was  $2.25 \text{ kWh m}^{-3}$  and  $3.83 \text{ kWh m}^{-3}$  respectively.  
 376 These values increased to  $2.74 \text{ kWh m}^{-3}$  and  $4.46 \text{ kWh m}^{-3}$  when the membrane aeration was  
 377 kept at its original value of  $84 \text{ Nm}^3\text{h}^{-1}$ .

### 378 379 3.4 Model application for optimisation

380 Results from the scenario analysis were used in the selection of better operational parameter  
 381 values (Table 5). The higher wastage rate (and lower SRT) resulted in a modest decline in  
 382 MLSS and higher F/M ratio, which previous studies have indicated may increase the sludge  
 383 fouling propensity (Trussell *et al.*, 2006). However, data collected on the real MBR over a  
 384 period corresponding to approximately twice the SRT indicated permeability to be maintained  
 385 at the levels achieved in the original without changing the cleaning regime, notwithstanding  
 386 the reduction in membrane aeration rate. This is attributable to the low operational fluxes ( $10\text{--}$   
 387  $13 \text{ l m}^{-2}\text{h}^{-1}$ ), well below the operating flux values for most large-scale MBRs. However, the  
 388 lower membrane aeration set point corresponded to a  $SAD_m$  of  $0.3 \text{ Nm}^3\text{m}^{-2}\text{h}^{-1}$ , which is still  
 389 within the range of  $SAD_m$  values ( $0.2 - 1.28 \text{ Nm}^3\text{m}^{-2}\text{h}^{-1}$ ) typically considered sufficient for  
 390 sustainable operation, even at higher fluxes (Judd, 2006). Changing the parameter values  
 391 did not compromise the effluent quality in terms of COD and N removal based on data

392 obtained through twice weekly grab sampling, but biological P removal deteriorated due to  
393 the increased recirculation ratio, as predicted by the model.

394  
395 Table 5 also displays the resulting energy saving compared to the original values. A  
396 substantial reduction in energy consumption per  $\text{m}^3$  of permeate produced was achieved  
397 (23%), and this value was predicted by the model within 5-10%. The energy consumption  
398 value of  $3.11 \text{ kWh}\cdot\text{m}^{-3}$  is at the lower end of values typically reported for small MBRs (Boehler  
399 *et al.*, 2007; Gnirss *et al.*, 2008), which can range from 3 to  $12 \text{ kWh}\cdot\text{m}^{-3}$  depending on the  
400 design and circumstances. However, this value is high when compared to larger, more  
401 efficient plants, which can be as low as  $0.62 \text{ kWh}\cdot\text{m}^{-3}$  for standard intermittent aeration  
402 (Garcés *et al.*, 2007). Other reported values for large-scale MBRs range from 0.6 to  $2.0$   
403  $\text{ kWh}\cdot\text{m}^{-3}$ , depending on operational parameters and flow conditions (Brepols *et al.*, 2009).

404  
405 The proposed modelling approach can be readily applied to other MBRs, even when  
406 operating under more stringent conditions, which is likely for larger scale plants, since it is  
407 widely reported that MBRs achieve good and consistent nutrient removal at lower HRT (*inter*  
408 *alia* Judd, 2006). However, operation at high HRTs is not uncommon for smaller plants, as  
409 indicated in Gnirss *et al.* (2008), and the findings of this paper may thus provide useful  
410 information for future design and operation of small scale installations. The extent of the  
411 reduction in energy consumption that can be achieved by applying the proposed  
412 methodology will depend on the influent wastewater composition, desired effluent quality,  
413 allowable MLSS range and SRT, and initial operating conditions.

414

#### 415 **4 Conclusions**

- 416 • A small MBR for domestic water recycling, running under unusual and challenging  
417 influent conditions, was dynamically modelled in ASM2d. The model provided an  
418 accurate prediction of the dynamic nutrient removal profile and MLSS concentrations  
419 using default ASM2d values for all biokinetic and stoichiometric parameters.
- 420 • A dedicated aeration model was used, incorporating the effect of elevated MLSS  
421 concentrations on oxygen transfer, and allowing differentiation between coarse and  
422 fine bubble aeration such that aeration demand could be accurately simulated.
- 423 • To allow realistic modelling of the plant, influent fractionation was carried out based  
424 on average influent concentrations obtained over a four-month sampling period.  
425 Analysis has shown the wastewater strength to be considerably higher than for a  
426 typical wastewater of entirely domestic origin with no dilution or infiltration. The  
427 amount of readily biodegradable substrate (45%) was also higher than typically  
428 reported values (20%) due to hydrolysis in the septic tank.
- 429 • A scenario analysis was conducted to simulate the effect of varying the SRT, the  
430 recirculation ratio and the DO set point on effluent quality, MLSS concentrations and  
431 aeration demand. Linking the outcomes with empirically-derived calculations for  
432 energy consumption allowed quantification and optimisation of the energy demand.  
433 Decreasing the membrane aeration flow and SRT had the most profound effect on  
434 total operational energy consumption, but there was a trade-off in achievable  $\text{NH}_4\text{-N}$   
435 removal due to diminished nitrification with decreasing SRT. Increasing the  
436 recirculation flow led to improved TN removal and to deterioration in TP removal. This  
437 modelling approach thus allows the operating envelope to be identified for meeting  
438 criteria based on energy demand and/or specific water quality determinants - and  
439 nutrients in particular.
- 440 • New operational parameter values were applied to the plant, resulting in an on-site  
441 reduction in energy consumption by 23%, without compromising effluent quality, as  
442 predicted by the model.

443

444 **Acknowledgements**

445 The authors are grateful to MOSTforWATER N.V. (Kortrijk, Belgium) for providing the  
 446 WEST® modelling software, and would also like to thank Thames Water for the resources  
 447 provided by them for this paper. Thomas Maere is supported by the Institute for  
 448 Encouragement of Innovation by means of Science and Technology in Flanders (IWT).  
 449 Lorenzo Benedetti is post-doctoral researcher of the Special Research Fund (BOF) of Ghent  
 450 University.  
 451

452 **References**

- 453 Abegglen, C., Ospelt, M. and Siegrist, H. (2008), "Biological nutrient removal in a small-scale  
 454 MBR treating household wastewater", *Water Research*, vol. 42, no. 1-2, pp. 338-346.
- 455 Boehler, M., Joss, A., Buetzer, S., Holzapfel, M., Mooser, H. and Siegrist, H. (2007),  
 456 "Treatment of toilet wastewater for reuse in a membrane bioreactor", *Water Science and*  
 457 *Technology*, vol. 56, no. 5.
- 458 Brepols, C., Schäfer, H. and Engelhardt, N. (2009), "Economic aspects of large scale  
 459 membrane bioreactors", *Final MBR-Network Workshop: "Salient outcomes of the European*  
 460 *projects on MBR technology"*, 31/03/2009 - 01/04/2009, Berlin, Germany.
- 461 Cicek, N., Macomber, J., Davel, J., Suidan, M. T., Audic, J. and Genestet, P. (2001), "Effect  
 462 of solids retention time on the performance and biological characteristics of a membrane  
 463 bioreactor", *Water Science and Technology*, vol. 43, no. 11, pp. 43-50.
- 464 Copp, J. B. (2002), "The COST Simulation Benchmark - Description and Simulator Manual."  
 465 Office for Official Publications of the European Communities, Luxembourg.
- 466 Dochain, D. and Vanrolleghem, P. A. (2001), "Dynamical Modelling and Estimation in  
 467 Wastewater Treatment Processes", IWA Publishing, London, UK.
- 468 EPA (2004). "Guidelines for Water Reuse", US Environmental Protection Agency.  
 469 EPA/625/R-04/108.
- 470 Erftverband (2001), "Weitergehende Optimierung einer Belebungsanlage mit  
 471 Membranfiltration – Zwischenbericht (Advanced optimisation of an activated sludge plant with  
 472 membrane filtration – mid-term report)", Report to the Ministry of Environment North-Rine  
 473 Westphalia, Germany, Erftverband Bergheim, pp. 73-93.
- 474 Erftverband (2004), "Optimierung einer Belebungsanlage mit Membranfiltration – Band 3  
 475 (Optimisation of an activated sludge plant with membrane filtration – volume 3)". Report to  
 476 the Ministry of Environment North-Rine Westphalia, Germany, Erftverband Bergheim, pp. 73-  
 477 93.
- 478 Fenu, A., Guglielmi, G., Jimenez, J., Sperandio, M., Saroj, D, Brepols, C., Lesjean, B. and  
 479 Nopens, I. (2010) "ASM-based biological modelling of MBR processes: A critical review with  
 480 a special regard to MBR specificities", Submitted for publication in *Water Research*.
- 481 Fletcher, H., Mackley, T. and Judd, S. (2007), "The cost of a package plant membrane  
 482 bioreactor", *Water research*, vol. 41, no. 12, pp. 2627-2635.
- 483 Garcés, A., De Wilde, W., Thoeye, C. and De Gueldre, G. (2007), "Operational cost  
 484 optimisation of MBR Schilde" *Proceedings of the 4th IWA International Membranes*  
 485 *Conference "Membranes for Water and Wastewater Treatment"*, 15-17 May 2007, Harrogate,  
 486 UK.
- 487 Germain, E., Nelles, F., Drews, A., Pearce, P., Kraume, M., Reid, E., Judd, S. J. and  
 488 Stephenson, T. (2007), "Biomass effects on oxygen transfer in membrane bioreactors",  
 489 *Water research*, vol. 41, no. 5, pp. 1038-1044.
- 490 Gernaey, K. V. and Jørgensen, S. B. (2004), "Benchmarking combined biological  
 491 phosphorus and nitrogen removal wastewater treatment processes", *Control Engineering*  
 492 *Practice*, vol. 12, no. 3, pp. 357-373.

- 493 Gnirss, R., Vocks, M., Stueber, J., Luedicke, C. and Lesjean, B. (2008), "Membrane  
494 Technique in a Freight Container for Advanced Nutrients Removal - The ENREM  
495 Demonstration Project", *IWA World Water Conference and Exhibition 2008*, 7-12 September  
496 2008, Vienna, Austria.
- 497 Henze, M., van Loosdrecht, M., Ekama, G. A. and Brdjanovic, D. (2008), "Biological  
498 Wastewater Treatment: Principles, Modelling and Design". IWA Publishing, London.
- 499 Henze, M., Gujer, W., Mino, T., Matsuo, T., Wentzel, M. C., Marais, G. v. R. and Van  
500 Loosdrecht, M. C. M. (1999), "Activated Sludge Model No.2d, ASM2d", *Water Science and  
501 Technology*, vol. 39, no. 1, pp. 165-182.
- 502 Henze, M., Gujer, W., Mino, T., van Loosdrecht, M. (2000), "Activated Sludge Models ASM1,  
503 ASM2, ASM2d and ASM3", IWA Publishing, London.
- 504 Jiang, T., Kennedy, M. D., Guinzbourg, B. F., Vanrolleghem, P. A. and Schippers, J. C.  
505 (2005), "Optimising the operation of a MBR pilot plant by quantitative analysis of the  
506 membrane fouling mechanism", *Water Science And Technology*, vol. 51, no. 6-7, pp. 19-25.
- 507 Jiang, T., Myngheer, S., De Pauw, D. J. W., Spanjers, H., Nopens, I., Kennedy, M. D., Amy,  
508 G. and Vanrolleghem, P. A. (2008), "Modelling the production and degradation of soluble  
509 microbial products (SMP) in membrane bioreactors (MBR)", *Water research*, vol. 42, no. 20,  
510 pp. 4955-4964.
- 511 Judd, S. (2006), "The MBR book : principles and applications of membrane bioreactors in  
512 water and wastewater treatment", 1st ed, Elsevier, Amsterdam; Boston; London.
- 513 Krampe, J. and Krauth, K. (2003), "Oxygen transfer into activated sludge with high MLSS  
514 concentrations", *Water Science And Technology*, vol. 47, no. 11, pp. 297-303.
- 515 Levenspiel, O. (1998), "Chemical Reaction Engineering", Third edition, John Wiley and Sons,  
516 Inc., Hoboken, NJ, USA.
- 517 Lobos, J., Wisniewski, C., Heran, M. and Grasmick, A. (2005), "Effects of starvation  
518 conditions on biomass behaviour for minimization of sludge production in membrane  
519 bioreactors", *Water Science and Technology*, vol. 51, no. 6-7, pp. 35.
- Lubello, C., Caffaz, S., Gori, R., & Munz, G. (2009). A modified activated sludge model to  
estimate solids production at low and high solids retention time. *Water Research*, 43(18),  
4539-4548.
- 520 Maere, T., Verrecht, B., Benedetti, L., Pham P.T., Judd, S. J. and Nopens, I. (2009),  
521 "Building a Benchmark Simulation Model to Compare Control Strategies for Membrane  
522 Bioreactors: BSM-MBR", *5th IWA specialised membrane technology conference for water &  
523 wastewater treatment*, 01-03 September 2009, Beijing, China.
- Manser, R., Gujer, W. and Siegrist, H. (2005). Consequences of mass transfer effects on the  
kinetics of nitrifiers. *Water Research*, 39(19), 4633-4642.
- 524 Metcalf and Eddy, Tchobanoglous, G., Burton, F. L. and Stensel, H. D. (2003), "Metcalf and  
525 Eddy - Wastewater Engineering – Treatment and Reuse", 3rd edition, McGraw-Hill, New  
526 York.
- 527 Munz, G., De Angelis, D., Goria, R., Moric, G., Casarci, M., Lubello, C. (2008), "Process  
528 efficiency and microbial monitoring in MBR and conventional activated sludge process  
529 treatment of tannery wastewater", *Bioresource Technology*, vol. 99, pp. 8559-8564.
- 530 Roeleveld, P. J. and Van Loosdrecht, M. C. M. (2002), "Experience with guidelines for  
531 wastewater characterisation in The Netherlands", *Water Science and Technology*, vol. 45,  
532 no. 6, pp. 77-87.
- Spérandio, M., and Espinosa, M. C. (2008). "Modelling an aerobic submerged membrane  
bioreactor with ASM models on a large range of sludge retention time". *Desalination* vol. 231,  
no. 1-3, pp. 82-90.
- 533 Stenstrom, M.K. and Rosso, D. (2008) "Aeration and mixing", Chapter in "Biological  
534 Wastewater Treatment: Principles, Modelling and Design", Henze, M., van Loosdrecht, M.,  
535 Ekama, G. A. and Brdjanovic, D. (2008), IWA Publishing, London.

- 536 Trussell, R. S., Merlo, R. P., Hermanowicz, S. W. and Jenkins, D. (2006), "The effect of  
537 organic loading on process performance and membrane fouling in a submerged membrane  
538 bioreactor treating municipal wastewater", *Water research*, vol. 40, no. 14, pp. 2675-2683.
- 539 Vanhooren, H., Meirlaen, J., Amerlink, Y., Claeys, F., Vangheluwe, H., Vanrolleghem, P.A.,  
540 2003. "WEST: Modelling biological wastewater treatment", *Journal of Hydroinformatics* 5 (1),  
541 27-50.
- 542 Vanrolleghem, P., Insel, G., Petersen, B., Sin, G., De Pauw, D., Nopens, I., Dovermann, H.,  
543 Weijers, S. and Gernaey, K. (2003) "A comprehensive model calibration procedure for  
544 activated sludge models", Proceedings of WEFTEC03.
- 545 Verrecht, B., Judd, S., Guglielmi, G., Brepols, C. and Mulder, J. W. (2008), "An aeration  
546 energy model for an immersed membrane bioreactor", *Water research*, vol. 42, no. 19, pp.  
547 4761-4770.
- 548 VSA (2005), "Leitfaden Abwasser im landlichen Raum - Wastewater in the rural  
549 environment", Swiss Water Pollutant Control Association, Zurich, Switzerland.
- 550 Wen, X., Xing, C. and Qian, Y. (1999), "A kinetic model for the prediction of sludge formation  
551 in a membrane bioreactor", *Process Biochemistry*, vol. 35, no. 3-4, pp. 249-254.
- 552 Yoon, S., Kim, H. and Yeom, I. (2004), "The optimum operational condition of membrane  
553 bioreactor (MBR): cost estimation of aeration and sludge treatment", *Water research*, vol. 38,  
554 no. 1, pp. 37-46.
- 555 Zaveri, R. M. and Flora, J. R. V. (2002), "Laboratory septic tank performance response to  
556 electrolytic stimulation", *Water research*, vol. 36, no. 18, pp. 4513-4524.

557

558 Table 1: Plant dimensions and operational parameters during the tracer test

Parameter	Unit	Value
Anoxic zone		
Volume anoxic zone	m <sup>3</sup>	10.09
Aerobic zone / MBR		
Membrane surface	m <sup>2</sup>	139.2
Membrane flux during filtration	l m <sup>-2</sup> h <sup>-1</sup>	10.78
Filtration time	s	600
Relaxation time	s	30
Backwash time	s	30
Backwash flux	l m <sup>-2</sup> h <sup>-1</sup>	10.78
Minimum tank volume	m <sup>3</sup>	12.21
Maximum tank volume	m <sup>3</sup>	12.78
Recirculation flow	m <sup>3</sup> d <sup>-1</sup>	57.6

559

560 Table 2: Average characteristics of influent to the MBR (after septic tanks + screening; samples taken  
561 twice per week from January to May 2009)

Variable	Unit	Average	St.Dev.	Variable	Unit	Average	St.Dev.
BOD <sub>5</sub>	mg l <sup>-1</sup>	228.17	21.31	TON	mg l <sup>-1</sup>	0.30	0.00
BOD <sub>f</sub>	mg l <sup>-1</sup>	114.60	14.37	NO <sub>2</sub> -N	mg l <sup>-1</sup>	0.02	0.01
COD	mg l <sup>-1</sup>	480.50	36.67	PO <sub>4</sub> -P	mg l <sup>-1</sup>	9.29	0.41
COD <sub>f</sub>	mg l <sup>-1</sup>	247.67	48.11	TP	mg l <sup>-1</sup>	10.87	0.54
TN	mg l <sup>-1</sup>	81.58	3.51	SS	mg l <sup>-1</sup>	107.32	9.29
ON	mg l <sup>-1</sup>	12.21	3.31	pH	-	7.14	0.09
NH <sub>4</sub> -N	mg l <sup>-1</sup>	69.10	5.52				

562

563 Table 3: Treatment plant wastewater fractionation vs. typical wastewater composition (Henze et al.,  
564 1999)

MBR influent composition in this study (COD=480 mg l <sup>-1</sup> , TKN=81 mg l <sup>-1</sup> , TP=11 mg l <sup>-1</sup> )				Typical wastewater composition (COD=260 mg l <sup>-1</sup> , TKN=25 mg l <sup>-1</sup> , TP=6 mg l <sup>-1</sup> )	
<i>Soluble</i>					
Variable	Unit	Value	% of tCOD	Value	% of tCOD
S <sub>F</sub>	mg l <sup>-1</sup>	126.86	26.4%	30	11.5%
S <sub>A</sub>	mg l <sup>-1</sup>	88.89	18.5%	20	7.7%
S <sub>NH4</sub>	mg l <sup>-1</sup>	69.10	-	16	-
S <sub>PO4</sub>	mg l <sup>-1</sup>	9.29	-	3.6	-
S <sub>I</sub>	mg l <sup>-1</sup>	21.56	4.5%	30	11.5%
<i>Particulate</i>					
Variable	Unit	Value	% of tCOD	Value	% of tCOD
X <sub>I</sub>	mg l <sup>-1</sup>	41.57	8.7%	25	9.6%
X <sub>S</sub>	mg l <sup>-1</sup>	191.26	39.8%	125	48.1%

565

\* Symbols used according to Henze et al., 1999

566

567

568

569 Table 4: Steady state simulation results compared with average measured values

Parameter	Units	Measured Values	- Default ASM2d values - (Henze et al., 1999)		- Default ASM2d values (Henze et al., 1999)	
			- Bio-P module (Gernaey and Jørgensen, 2004)		- Bio-P module (Gernaey and Jørgensen, 2004)	
					- $\mu_{PAO} = 2 \text{ d}^{-1}$	
					- $b_{PAO} = 0.1 \text{ d}^{-1}$	
					- $Y_{PO} = 0.2 \text{ gP} \cdot (\text{g COD})^{-1}$	
$NH_4-N$	$\text{g m}^{-3}$	0.07	0.337		0.338	
$NO_3-N$	$\text{g m}^{-3}$	21.4	21.9		21.68	
$PO_4-P$	$\text{g m}^{-3}$	4.35	9.65		5.18	
MLSS	$\text{g m}^{-3}$	7,832	6,584		7,869	

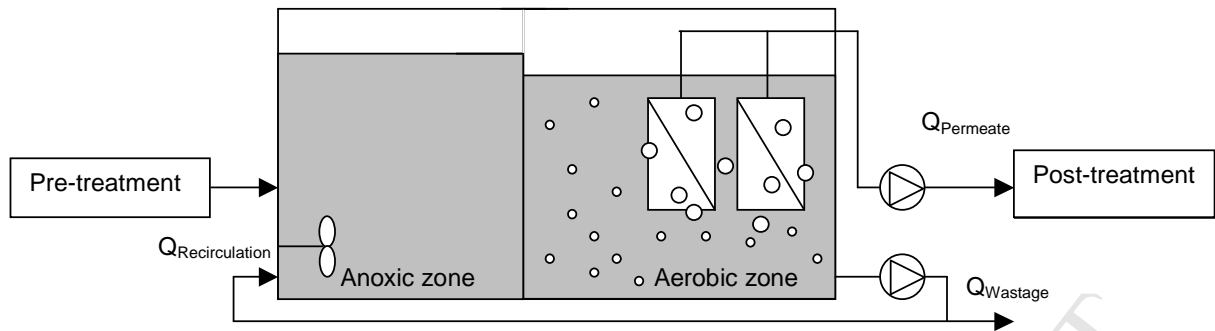
570

571

572 Table 5: Changes in operational parameter values according to the conclusions from the scenario  
 573 analysis, and comparison in energy consumption between original and optimised system (energy  
 574 demand of membrane aeration, activated sludge aeration, mixing of anoxic zone, permeate pump and  
 575 recirculation pump)

	Unit	Original	New
<b>Operational parameters</b>			
Membrane aeration	$\text{Nm}^3 \cdot \text{hr}^{-1}$	84	42
Wastage rate	$\text{m}^3 \cdot \text{d}^{-1}$	0.485	0.645
<i>i.e. SRT</i>	d	47	35
DO set-point	$\text{mg l}^{-1}$	2	1.25
Recirculation flow	$\text{m}^3 \cdot \text{d}^{-1}$	57.6	108
<i>i.e. Recirculation ratio</i>	-	2.27	4.25
<b>Energy consumption</b>			
Measurement	$\text{kWh m}^{-3}$	4.03	3.11
Reduction	%		23%
Model prediction	$\text{kWh m}^{-3}$	4.25	2.99
Deviation from real value	%	5.1	3.9

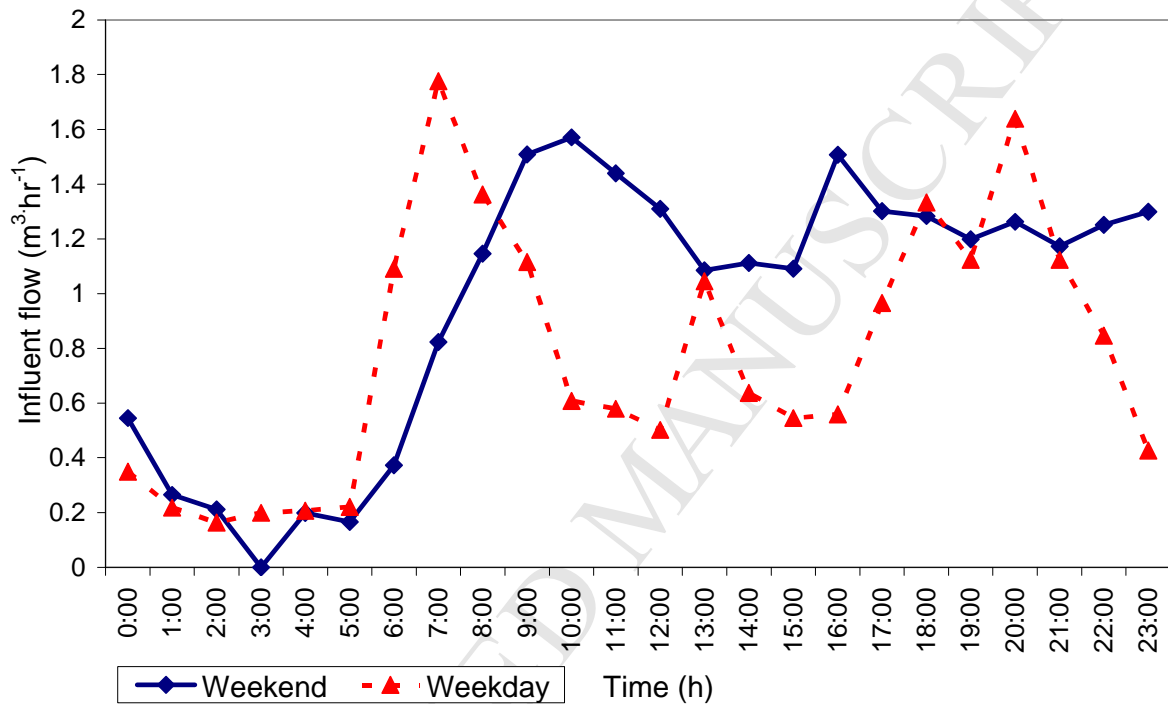
576



577

578

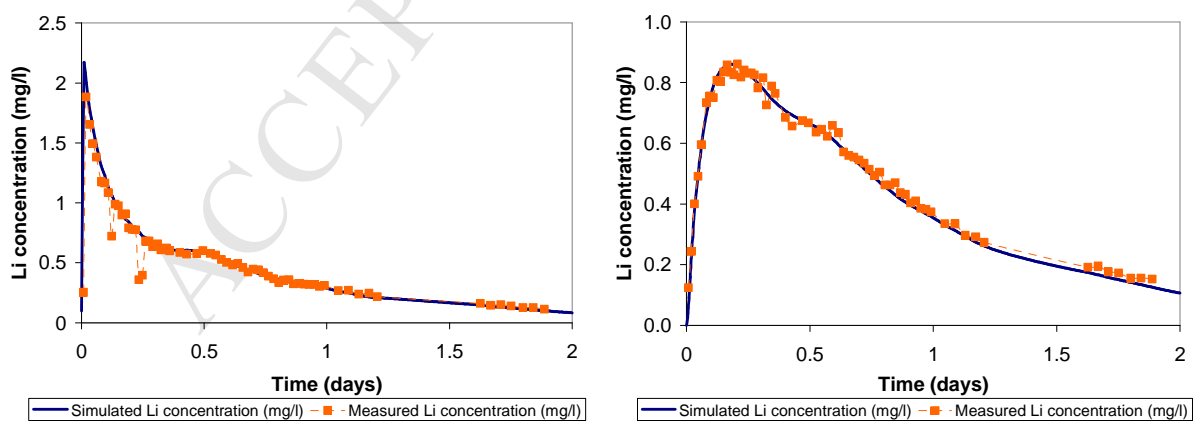
Figure 1: Schematic overview of the wastewater recycling plant



579

580

Figure 2: Comparison of typical diurnal flow profiles during a weekday and a day in the weekend



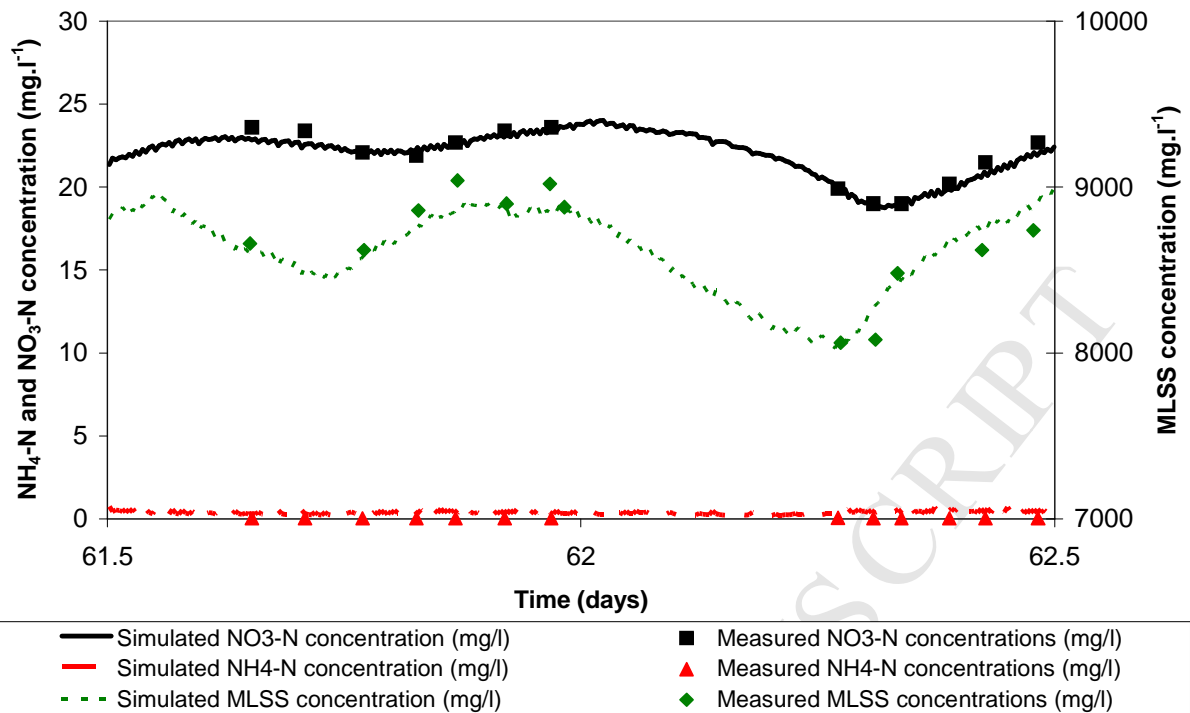
581

582

583

Figure 3: Predicted and actual Li concentrations in (a) anoxic, and (b) aerobic tanks during the tracer test



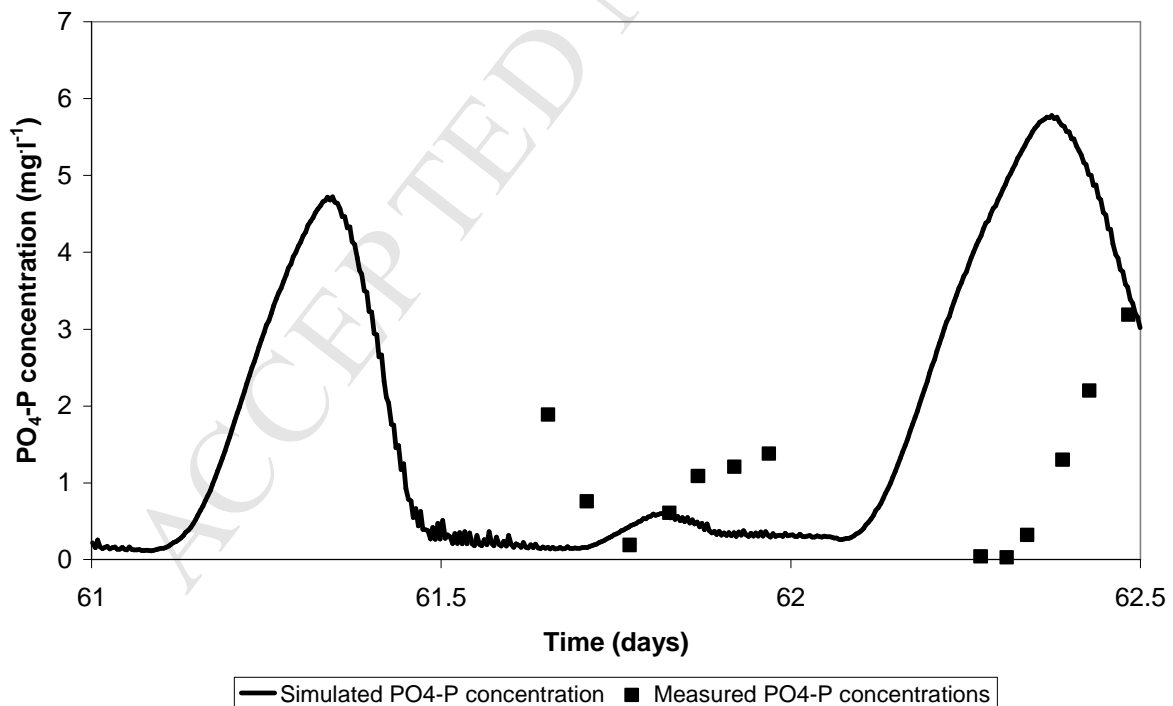


584

585 Figure 4: Simulated and recorded  $\text{NH}_4\text{-N}$ ,  $\text{NO}_3\text{-N}$  and MLSS concentrations using measured  $Q_{\text{air, fine}}$   
 586 averaged per 15 minute interval, as input

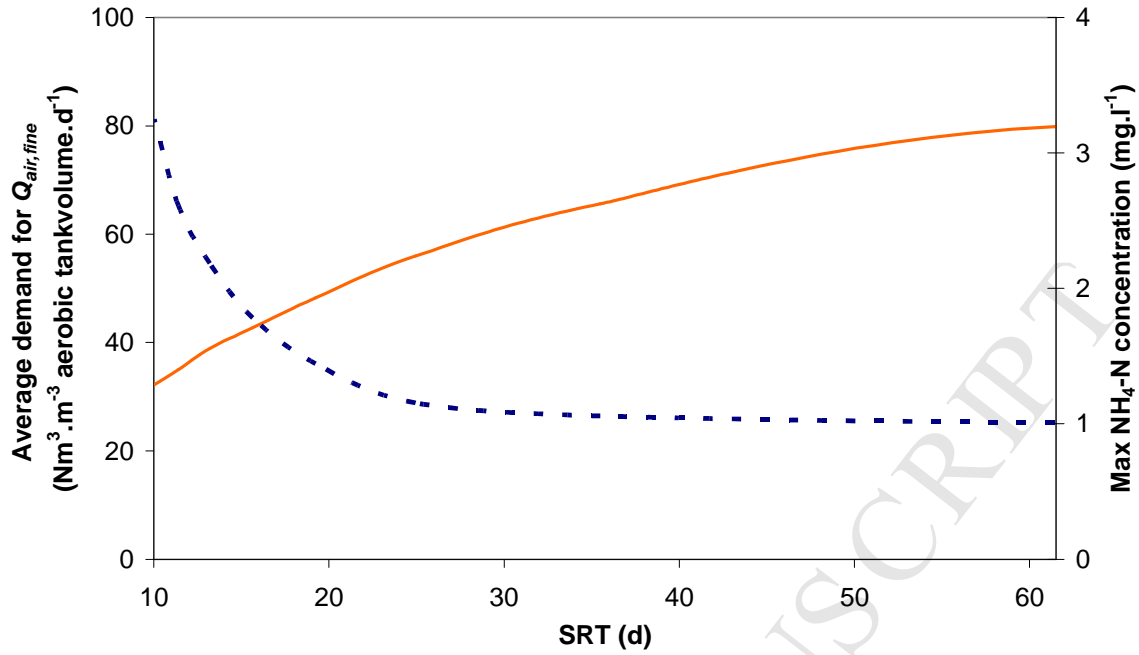
587

588



589

590 Figure 5: Simulated and measured  $\text{PO}_4\text{-P}$  values using measured measured  $Q_{\text{air, fine}}$  averaged per 15  
 591 minute interval, as input



592

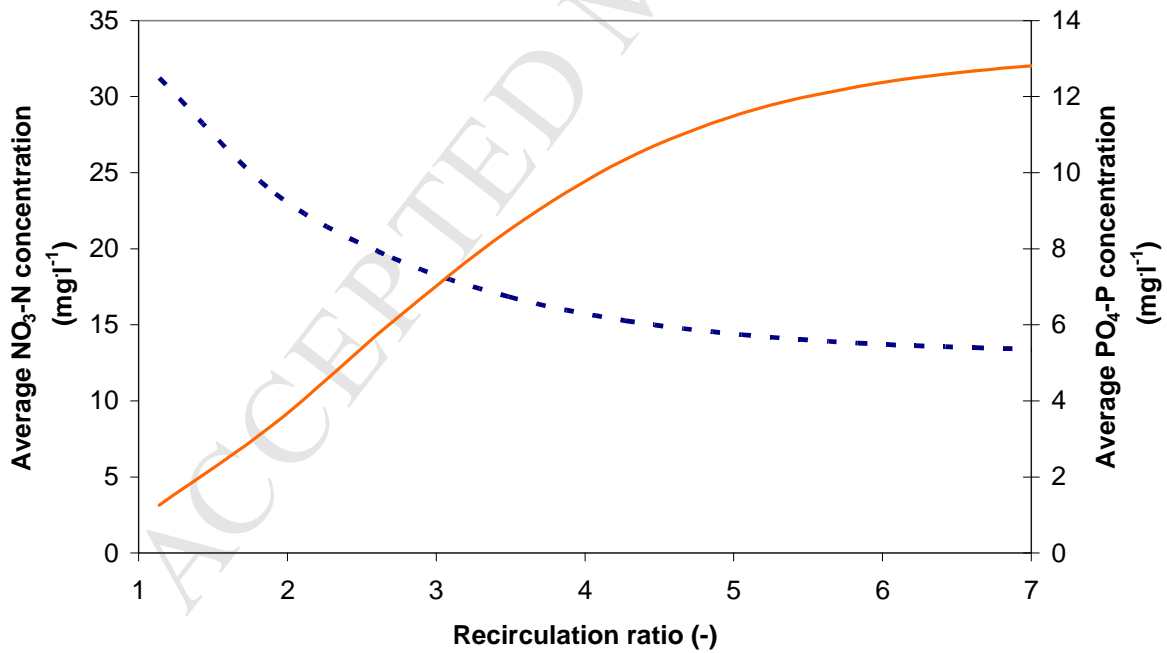
593

594

595

596

Figure 6: Influence of wastage rate on the total demand for biology aeration ( $Q_{air, fine}$ ) and the maximum occurring effluent  $NH_4-N$  concentration during the 35-day simulation ( $Q_{air, coarse} = 42 Nm^3 \cdot h^{-1}$ ; DO setpoint =  $1.25 mg \cdot l^{-1}$ ; recirculation flow =  $108 m^3 \cdot d^{-1}$ )

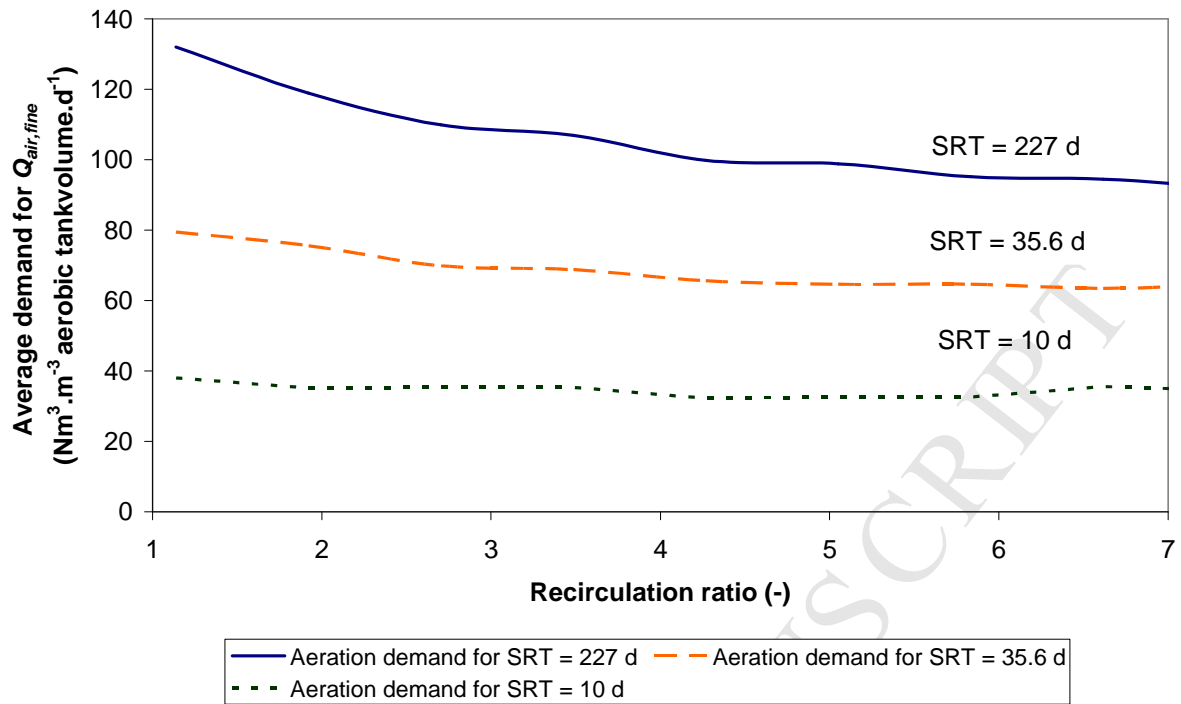


597

598

599

Figure 7: Influence of recirculation flow rate on the average effluent  $NO_3-N$  and  $PO_4-P$  concentrations during the 35-day simulation ( $Q_{air, coarse} = 42 Nm^3 \cdot h^{-1}$ ; DO setpoint =  $1.25 mg \cdot l^{-1}$ )



600

601 Figure 8: Influence of recirculation rate and SRT on total demand for  $Q_{air, fine}$  ( $Q_{air, coarse} = 42 \text{ Nm}^3 \cdot \text{h}^{-1}$ ; DO  
 602 setpoint =  $1.25 \text{ mg} \cdot \text{l}^{-1}$ )

603